

# Nonlinear pressure-velocity waveforms in large arteries, shock waves and wave separation

Oleg Ilyin

*Dorodnicyn Computing Center of Federal Research Center Computer Science and Control  
of RAS, Vavilova 40, Moscow, 119333, Russia*

---

## Abstract

Nonlinear inviscid 1D blood flow equations were studied analytically using the method of characteristics. The initial-boundary value problem for a class of the initial-boundary conditions (including a triangle-shaped profile) at the aortic outlet was considered. The nonlinear pressure-velocity profile and shock conditions were derived as closed analytical expressions with second order accuracy on the relative luminal area change. Finally, the fully nonlinear wave separation expressions were obtained using the Riemann invariants. The results show good correspondence with the data from the literature.

*Keywords:* Biological fluid dynamics, nonlinear waves

---

## 1. Introduction

The most popular 1D hemodynamic pressure-velocity propagation models are based on the quasilinear partial differential equations of the hyperbolic type [1]-[3]. The equations describe blood motion in distensible vessels in terms of unknown pressure and blood velocity (or the vessel's cross-sectional area and blood velocity). Solutions to 1D equations are usually obtained numerically for the branching arterial network [4]-[8] and they can be coupled with the solutions of the full 3D Navier-Stokes equations [9]. As the difference  $\Delta A$  between the systolic luminal area  $A_1$  and the diastolic  $A_0$  is small ( $\Delta A/A_0$  is assumed to be negligible) the equations can be linearized around  $A_0$ . The reduced equations are well known in sound propagation theory [10]. The linear theory allows the assessment of several properties of the flow which are important for the estimation of cardiovascular risk. Any change in the geometry of a vessel (bifurcation, lumen narrowing and other factors changing vascular impedance) causes an appearance of reflected waves. Simple and concise formulas for the wave separation into the forward and backward waves can be obtained in the framework of the linear theory using the wave separation analysis [11]-[14] or wave intensity analysis [13]-[15].

---

*Email address:* oilyin@gmail.com (Oleg Ilyin)

The perturbations travel along the constant and parallel characteristics in the linear approximation and hence the waves do not change their initial form and shock-waves do not appear. Nevertheless, the nonlinear effects can play a significant role in the behaviour of the pressure-velocity waves. For instance, if the reported difference between the diameters of large vessels like the carotid artery in systole and diastole is 10% [16], then the relative difference between the lumen areas are about  $\Delta A/A_0 \approx 0.2$ . Therefore, a full nonlinear analysis should be performed. The existence of shock-waves has been proven numerically in [17], while the formation of shock waves at a distances between few centimetres and several meters from the aortic outlet (depending on the elastic properties) has been reported in [18]. The possibility of roll waves in collapsible tubes has been considered in [19]. The effects of friction coupled with nonlinearities has been studied in [21]-[22].

The goal of the paper is to derive the closed analytical expression for the blood pressure, the luminal area and the velocity using the nonlinear equations for the mass and moment transfer. The flow is considered to be inviscid, while the viscoelastic terms in the wall-pressure response are excluded and the unperturbed luminal area is constant within the vessel. In contrast to the linear theory, where  $\Delta A/A_0$  is assumed to be negligible, we will include these terms but exclude quadratic terms  $(\Delta A/A_0)^2$ . In other words, the obtained solutions include  $(\Delta A/A_0)^2$  error in comparison to the exact solutions of the mass and moment transfer equations. The simplified nonlinear assumption allows the main features of the nonlinear theory to be included as the characteristics can converge or diverge. The analytical expression for the pressure-velocity waves for a class of the initial-boundary conditions is derived providing quantitative information about the evolution of waves in time and space. It is shown that the wave significantly changes its shape while traveling along a vessel and shock waves can emerge. Moreover, with the use of the Riemann invariants the closed nonlinear wave separation formulae were calculated, the analytical expressions for the forward and backward waves were obtained.

## 2. The mass and momentum conservation equations and their reduction in the case of sole wave

Consider the mass and momentum conservation equations for inviscid blood motion in a distensible vessel with impermeable walls [3]

$$\frac{\partial A}{\partial t} + \frac{\partial Q}{\partial x} = 0, \quad \frac{\partial Q}{\partial t} + \frac{\partial}{\partial x} \left( \frac{\alpha Q^2}{A} \right) = -\frac{A}{\rho} \frac{\partial p}{\partial x}, \quad (1)$$

where  $Q, A$  are the flow, the cross-section area of a vessel respectively,  $\alpha$  is the profile shape factor assumed to be equal unity (the flow is flat) and  $\rho$  is the blood density.

We introduce the distensibility  $D(A)$  which is by the definition [3]

$$D(A) = \frac{1}{A} \frac{dA}{dp}. \quad (2)$$

We assume that distensibility  $D(A)$  is a known function of  $A$ . In most applications this relationship is as follows

$$D(A) = \frac{D_0}{A^n}, \quad n > 0.$$

Integrating the expression (2) we obtain

$$p = p_0 + \frac{1}{nD_0}(A^n - A_0^n), \quad (3)$$

where  $A_0$  is the undisturbed luminal area  $p_0$  is the corresponding blood pressure. Additional information about pressure-area relationship and the Hooke law could be found in the Appendix.

For a flat velocity profile ( $\alpha = 1$ ) we use  $Q = uA$ . In terms of  $u, A$  the equations (1) have the form

$$\frac{\partial A}{\partial t} + u \frac{\partial A}{\partial x} + A \frac{\partial u}{\partial x} = 0, \quad \frac{\partial u}{\partial t} + \frac{1}{\rho D(A) A} \frac{\partial A}{\partial x} + u \frac{\partial u}{\partial x} = 0. \quad (4)$$

For a sole forward traveling wave we have the following relationship between the area of the vessel and the velocity (see paragraph 4)

$$u = \int_{A_0}^A \frac{dz}{\sqrt{\rho D(z)} z}, \quad (5)$$

where  $A_0$  is the undisturbed vessel cross-sectional area (for the backward traveling wave we substitute  $u = - \int_{A_0}^A \frac{dz}{\sqrt{\rho D(z)} z}$ ). If we substitute the expression (5) in the system (4) then the both equations in (4) will have the same form, hence the system of the partial differential equations reduce to only one equation

$$\frac{\partial A}{\partial t} + \left( \int_{A_0}^A \frac{dz}{\sqrt{\rho D(z)} z} + \frac{1}{\sqrt{\rho D(A)}} \right) \frac{\partial A}{\partial x} = 0.$$

Taking into account that  $D(A) = D_0/A^n$  we finally obtain the equation for the forward wave

$$\frac{\partial A}{\partial t} + \frac{1}{\sqrt{\rho D_0}} \left( \left(1 + \frac{2}{n}\right) A^{n/2} - \frac{2}{n} A_0^{n/2} \right) \frac{\partial A}{\partial x} = 0. \quad (6)$$

The analytical solution to this equation in an implicit form is presented in Appendix 2.

### 3. Analytical nonlinear area-pressure wave and shock wave conditions

The equation (6) can be reduced to the following (see details below)

$$\frac{\partial A}{\partial t} + c_0 \left( 1 + \frac{n+1}{2A_0} (A - A_0) \right) \frac{\partial A}{\partial x} = 0, \quad (7)$$

where  $c_0 = \sqrt{A_0^n/\rho D_0}$  is the pulse wave velocity in the linear theory. We supplement this equation with the following triangle-shaped initial-boundary condition (Fig. 2) at  $x = 0$  for  $t \in [0, T_0]$ , where  $T_0$  is one heartbeat

$$A(t, x)|_{x=0} = A_0 + at, \quad t \in [0, t_0], \quad (8)$$

$$A(t, x)|_{x=0} = A_0 + b(t_1 - t), \quad b \equiv \frac{at_0}{t_1 - t_0}, \quad t \in [t_0, t_1], \quad (9)$$

$$A(t, x)|_{x=0} = A_0, \quad t \in (t_1, T_0] \quad (10)$$

and

$$A(t, x)|_{t=0} = A_0, \quad x > 0. \quad (11)$$

In practice  $T_0 \approx 1s, t_1 \approx 0.3s$ . The conditions (8)-(9) correspond to systole and (10) to diastole. We do not consider the exponential drop of the cross-sectional area or pressure during diastole which is usually observed in clinical studies. This effect is a consequence of the resistance of the distal vasculature which is not included in the present investigation and the cross-sectional area is assumed to be constant.

The nonlinear study of blood motion equations with the use of the method of characteristics has been presented in several papers [20]-[24]. The analytical expression for the pressure-velocity (or the area-velocity) waves has not been presented before in the nonlinear case; our goal is to solve analytically the problem (7) and (8)-(11).

From Eq. (6) one can deduce that the nonlinear area-pressure pulse velocity  $c$  has the following form

$$c = \frac{1}{\sqrt{\rho D_0}} \left( \left( 1 + \frac{2}{n} \right) A^{n/2} - \frac{2}{n} A_0^{n/2} \right),$$

then the relative velocity (analog of the Mach number) is

$$\frac{u}{c} = \frac{2}{n} \frac{(A^{n/2} - A_0^{n/2})}{\left( 1 + \frac{2}{n} \right) A^{n/2} - \frac{2}{n} A_0^{n/2}},$$

where we have applied the expression (5) for the blood velocity  $u = \int_{A_0}^A \frac{ds}{\sqrt{\rho D(s)s}} = \frac{2(A^{n/2} - A_0^{n/2})}{n\sqrt{\rho D_0}}$ . If one assumes that the value of the perturbed cross-sectional area  $A$  is 20% larger than the unperturbed area  $A_0$  i.e.  $A/A_0 = 1.2$  and  $n = 0.5$  then the following result is obtained

$$\frac{u}{c} \approx 0.218,$$

therefore, similarly to the clinical measurements the flow is significantly subsonic.

The relative change of the cross-sectional is not small then this effect should be kept in the consideration. We expand the pulse velocity in Taylor series near

$A_0$ , keep only the linear perturbations and neglect quadratic  $((A/A_0)^2 \approx 1.04)$  and higher terms

$$c \approx c_0 \left( 1 + \frac{n+1}{2A_0}(A - A_0) \right), \quad (12)$$

where  $c_0 = \sqrt{A_0^n / \rho D_0}$  is the pulse wave velocity in the linear theory. Replacing the pulse wave velocity in Eq. (6) by its value from (12) we derive the equation (7). The solution to Eq. (7) can be constructed in the same way as for Eq. (6) (Appendix 2), we have

$$A - A_0 = a \left( t - \frac{x}{c_0(1 + \frac{n+2}{2A_0}(A - A_0))} \right),$$

where  $c_0 = \sqrt{A_0^n / \rho D_0}$  is the pulse wave velocity in the linear theory. Solving the quadratic algebraic equation for  $A - A_0$  we finally deduce that

$$A = A_0 + \frac{-(1 - akt) + \sqrt{(1 - akt)^2 - 4ak(c_0^{-1}x - t)}}{2k}, \quad (13)$$

where  $k \equiv \frac{n+2}{2A_0}$ . The expression (13) gives the solution of the considered problem for the boundary condition (8).

Similarly, the boundary condition (9) leads to the solution

$$A = A_0 + \frac{-(1 - bk(t_1 - t)) + \sqrt{(1 - bk(t_1 - t))^2 + 4bk(c_0^{-1}x + (t_1 - t))}}{2k}. \quad (14)$$

Now we need to obtain the conditions for the appearance of a shock wave. The shock wave appears when  $\frac{\partial A}{\partial t}, \frac{\partial A}{\partial x}$  are infinite. This happens when the denominator in  $\frac{\partial A}{\partial t}, \frac{\partial A}{\partial x}$  equals to zero. Then for (13) we have the curve  $C_s$

$$C_s : \quad x = \frac{c_0}{4ak}(1 + akt)^2.$$

We conclude that the shock wave appears for the first time  $t_s$  when the characteristic  $x = c_0 t$  crosses  $C_s$ . Then

$$1 + akt_s = \sqrt{4akt_s},$$

the solution of this algebraic equation is

$$t_s = \frac{1}{ka}$$

and finally

$$x_s = \frac{c_0}{ka} = \frac{2c_0 t_0}{(n+2)\frac{at_0}{A_0}} = \frac{2c_0 t_0}{(n+2)} \left( \frac{\Delta A}{A_0} \right)^{-1}, \quad (15)$$

where  $\Delta A = a_0 t_0$ . If we assume that  $c_0$  lies in the range from  $3 m/s$  to  $10 m/s$  and  $n = 0.5$ ,  $a t_0 \equiv \Delta A = 0.2 A_0$  where  $t_0 = 0.15 s$ , then we have for the distance of shock  $x_s$  the estimate  $4 c_0 t_0$  varying from  $1.8 m$  to  $6 m$ . This result is similar to the estimate from [18].

The detailed consideration of the wave dynamics after the appearance of the shock requires the full analysis of the characteristics and is presented below. For the sake of simplicity we set  $a = b$  for the boundary conditions (symmetric initial pulse) (8)-(9), we have  $A(t, x)|_{x=0} = A_0 + at$ ,  $t \in [0, t_0)$  and  $A(t, x)|_{x=0} = A_0 + a(2t_0 - t)$ ,  $t \in [t_0, 2t_0]$ . The solution along the characteristics is given by

$$A = f(s), \quad t(s) = \frac{1}{c_0(1 + k(f(s) - A_0))} x + s, \quad (16)$$

where  $s$  is a parameter (constant of integration), the function  $f(s)$  is unknown, we can find  $f(s)$  from the boundary condition. From the conditions at  $x = 0$  we deduce that  $f(s)$  equals  $A_0 + as$ ,  $s \in [0, t_0)$  and  $A_0 + a(2t_0 - s)$ ,  $s \in [t_0, 2t_0]$ . The shock wave  $X(t)$  appears if two characteristics (fixed by the parameters  $s = s_1, s = s_2$ ) intersect. Using (16) we have

$$X = c_0(1 + k(f(s_1) - A_0))(t - s_1), \quad X = c_0(1 + k(f(s_2) - A_0))(t - s_2). \quad (17)$$

We need to find three unknowns  $s_1, s_2, X$ , but only the two equations are introduced. The conditions above define all possible intersections between the characteristic lines, but we need to keep only a subset of the intersections which define a shock curve. Additional information about the shock wave velocity can be extracted from the equation (7). Integrating Eq. (7) on  $x$  we deduce that

$$\int_0^\infty (A(t, x) - A_0) dx$$

is conserving quantity (integral of motion) for  $t > t_1$ . This fact will be important in the further consideration of large  $t$  pulse wave asymptotics.

Eq. (7) can be rewritten in the following form consistent with the aforementioned integral of motion

$$\frac{\partial A}{\partial t} + \frac{\partial Q}{\partial x} = 0, \quad Q \equiv c_0(A - A_0) + \frac{c_0 k}{2}(A - A_0)^2.$$

Integration of this equation over  $x$  leads to the Hugoniot jump condition

$$\frac{dX}{dt} = \frac{Q_1 - Q_2}{A_1 - A_2},$$

where  $Q_1, Q_2$  and  $A_1, A_2$  are the values of the corresponding variables in the right and the left sides from the jump. Then the shock velocity equals

$$\begin{aligned} & \frac{dX}{dt} = \\ & = \frac{c_0(A(s_1) - A_0) + \frac{c_0 k}{2}(A(s_1) - A_0)^2 - (c_0(A(s_2) - A_0) + \frac{c_0 k}{2}(A(s_2) - A_0)^2)}{(A(s_1) - A_0) - (A(s_2) - A_0)} \end{aligned}$$

and we know that  $A(s_1) = f(s_1), A(s_2) = f(s_2)$ , finally

$$\frac{dX}{dt} = c_0 + \frac{c_0 k}{2} \{f(s_1) + f(s_2) - 2A_0\}. \quad (18)$$

Eqs (17) and (18) allow to express  $s_1, s_2$  via  $X$  and derive the closed differential equation for  $X(t)$ . The form of this equation depends on the selection of  $s_1, s_2$ . If  $s_1, s_2 \in [0, t_0)$  then from (17) we obtain

$$s_{1,2} = \frac{(akt - 1) \pm \sqrt{(1 + akt)^2 - \frac{4ak}{c_0} X}}{2ak}$$

and Eq. (18) takes the form

$$\frac{dX}{dt} = c_0 + \frac{c_0 k}{2} (akt - 1),$$

which has the solution  $X(t) = (x_0 - \frac{c_0}{4ak}) + \frac{c_0}{4ak} (1 + akt)^2$ , where  $x_0$  is constant of integration. The case  $s_2 = 0$  corresponds to the characteristic  $x = c_0 t$ , this characteristic intersects the shock  $X(t)$  at the point  $(t_s, x_s)$  (Figure 1), then at this point we have the additional constraint  $X(t_s) = c_0 t_s$  and we conclude that  $x_0 = \frac{c_0}{4ak}$ . Therefore, as anticipated, we recover the formula

$$C_s : X(t) = \frac{c_0}{4ak} (1 + akt)^2, \quad t \in [t_s, t_s^*], \quad (19)$$

which was obtained using the explicit forms of the wave fronts. Note that  $t_s = \frac{1}{ak}$  and  $t_s^* = \frac{1+2akt_0}{ak}$ , where  $t_s^*$  denotes the moment of time when the characteristic  $x = c_0(1 + kat_0)(t - t_0)$  meets the curve  $C_s$  (Fig. 1).

The remained case corresponds to the shock wave originated from the intersection of the characteristics  $s_1 \in [0, t_0), s_2 \in [t_0, 2t_0]$ . This case is more complicated. Similarly to the previous case we obtain for the velocity of the shock wave the equation

$$C_s : \frac{dX}{dt} = c_0 + \frac{c_0}{4a} \left\{ 2ak(t_0 + t) + \sqrt{(1 + akt)^2 + \frac{4ak}{c_0} X} - \sqrt{(1 + 2akt_0 - akt)^2 + \frac{4ak}{c_0} X} \right\}, \quad t > t_s^*. \quad (20)$$

The equation (20) can be investigated qualitatively. We can notice that the term in the curved brackets is positive for large  $t$ . Therefore, the distance between the characteristic with  $s = t_1 = 2t_0$  and the position of the shock is monotonically increasing since the propagation velocity of the shock (20) is greater than the velocity of the considered characteristic which equals  $c_0$ .

The asymptotic behavior of the solutions (20) can be also obtained. If  $t \rightarrow \infty$  then the difference between the square root terms tends to zero and then  $X_t = c_0 + \frac{c_0 k}{2} (t_0 + t)$ , the solution behaves as  $c_0(1 + \frac{kt_0}{2})t + \frac{c_0 k}{4} t^2$ .

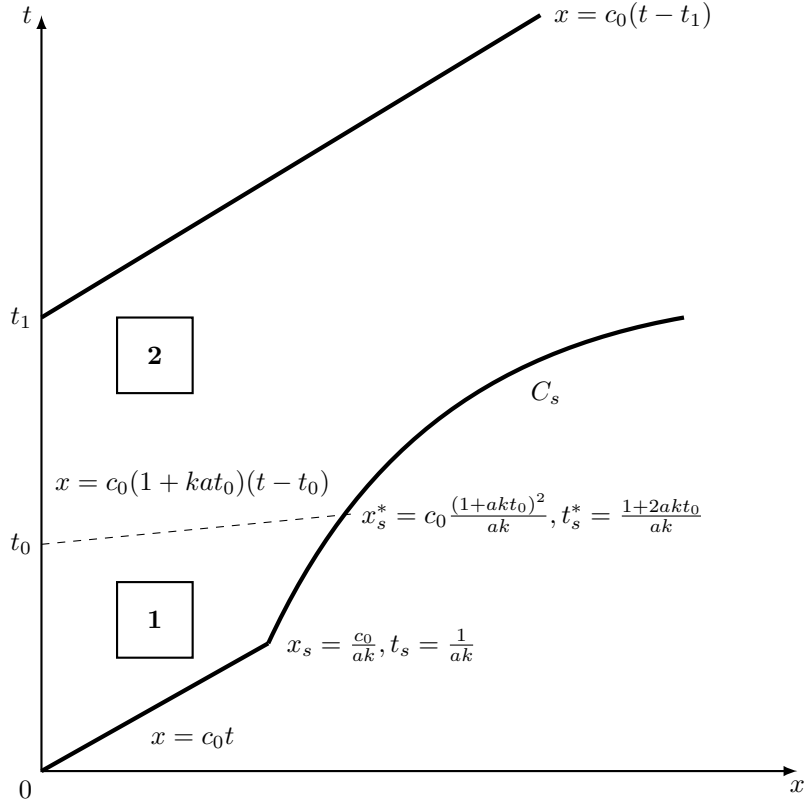


Figure 1: The characteristics for the problem (6)-(11). The domain 1 is bounded by the characteristics  $x = c_0 t$ ,  $x = c_0(1 + kat_0)(t - t_0)$  and the shock curve  $C_s$ , the domain 2 is bounded by the characteristics  $x = c_0(1 + kat_0)(t - t_0)$ ,  $x = c_0(t - t_1)$  and the shock curve  $C_s$ , where  $t_1$  is the systole duration,  $x = 0$  is the position of the aortic root,  $c_0$  is the pulse wave velocity in the linear theory. The shock wave lies on the curve  $C_s$ . The solutions are given by formulas (21)-(24) and remain unperturbed outside the domains 1 and 2.



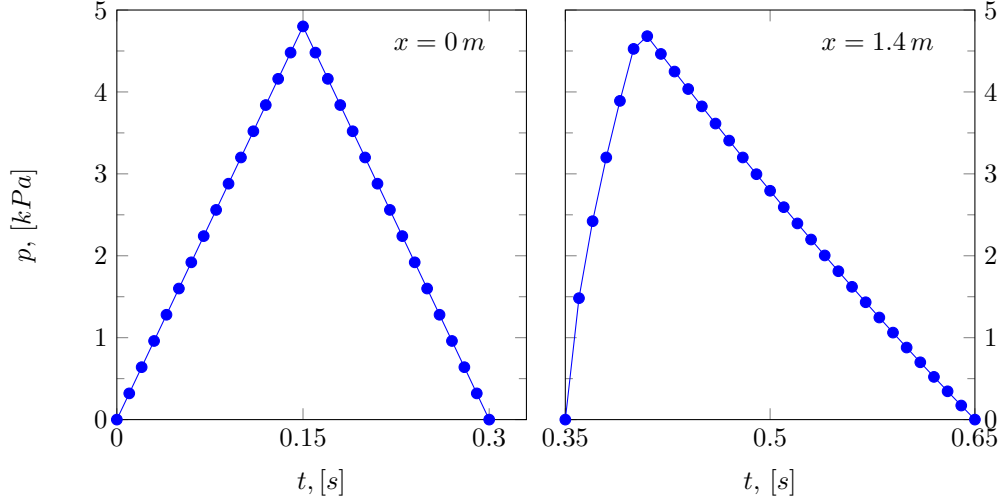


Figure 2: The initial symmetrical triangle shaped pulse-wave form at the aortic root (*left picture*) at the aortic root  $x = 0m$  significantly changes its form after the wave travels for the time period of  $0.35s$  and is measured at the point  $x = 1.4m$  (*right picture*). The initial pulse wave has the physiological duration of  $0.3s$ ,  $c_0 = 4m/s$  and  $n = 0.5$ , the unperturbed radius of the vessel equals  $1.5 * 10^{-2}m$ ,  $A_0 \approx 7 * 10^{-4}m^2$ . The non-symmetrical initial waves can be considered using the formulas (13)-(14).

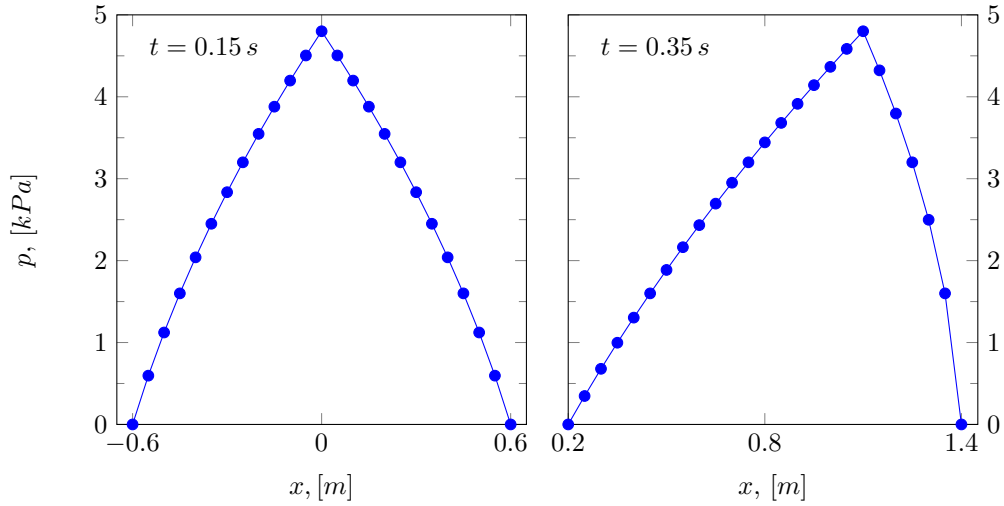


Figure 3: Two snapshots in time for the pressure pulse waves are presented. The aortic outlet is placed at  $x = 0$ . The pressure wave in the left slide is formally continued for  $x < 0$ . The initial pulse wave has the physiological duration of  $0.3s$  and  $c_0 = 4m/s$ ,  $n = 0.5$ , the unperturbed radius of the vessel equals  $1.5 * 10^{-2}m$ ,  $A_0 \approx 7 * 10^{-4}m^2$ . The non-symmetrical initial waves can be considered using the formulas (13)-(14).

This fact means that the length of the pulse wave tends to infinity for large  $t$  (infinitely stretched wave). Moreover, the maximum amplitude of the wave decreases and tends to  $A_0$  after appearance of the shock because  $\int_0^\infty (A - A_0)dx$  is conserving quantity.

The typical evolution of the waveform is presented in Fig. 2. and Fig. 3. Finally, compiling all the previous results we obtain the following proposition

*The problem (7)-(11) has the following solution*

$$A(t, x) = A_0 + \frac{-(1 - akt) + \sqrt{(1 - akt)^2 - 4ak(c_0^{-1}x - t)}}{2k}, \quad (21)$$

which is valid for  $t \geq 0, x \geq 0$  in the domain bounded by the characteristics  $x = c_0t, x = c_0(1 + kat_0)(t - t_0)$  and the part of the shock curve  $C_s$  given by the expression (19) (the domain 1 in Figure 1)

and

$$A = A_0 + \frac{-(1 - bk(t_1 - t)) + \sqrt{(1 - bk(t_1 - t))^2 + 4bk(c_0^{-1}x + (t_1 - t))}}{2k}, \quad (22)$$

which is valid for  $t \geq 0, x \geq 0$  in the domain bounded by the characteristics  $x = c_0(1 + kat_0)(t - t_0), x = c_0(t - t_1)$  and the part of the shock curve  $C_s$  given by the equation (20) in the case of the symmetrical initial pulse (the domain 2 in Figure 1). We have used the following definitions

$$k \equiv \frac{n + 2}{2A_0}, \quad c_0 \equiv \sqrt{A_0^2 / \rho D_0}.$$

Outside of the domains 1 and 2 the solution remains unperturbed,  $A = A_0$ . The blood velocity  $u$  is calculated from the linearized version of the formula (5)

$$u(t, x) = c_0 \frac{A - A_0}{A_0} \quad (23)$$

and

$$p(t, x) = p_0 + \rho c_0^2 \frac{A - A_0}{A_0}. \quad (24)$$

This solutions have the error of order  $O((\Delta A/A)^2)$  for  $n \neq 2$  and are exact for  $n = 2$ . The backward wave can be obtained from the formulas above by replacing  $c_0^{-1}x$  with  $-c_0^{-1}x$ .

Finally, let us mention one important fact. Since all the terms in the equations (1) (or (4)) depend on  $t, x$  only via  $p, A$  (or  $u, A$ ) then the solutions (21)-(23) are invariant on shifts

$$(t, x) \rightarrow (t + t_0, x + x_0). \quad (25)$$

The values of  $t_0, x_0$  are arbitrary constants. For the practical needs they can be used for fitting the experimental waveforms. Using the symmetry (25) the solutions with non-triangular wave forms at the aortic root can be easily obtained from the solutions (21)-(24) simply by replacing  $t, x$  with  $t + t_0, x + x_0$ .

#### 4. Exact Nonlinear Wave-Separation Formulas

We will derive the closed analytical expression for the separation of a pressure wave measured in an artery into a forward and backward (reflected wave) components using the Riemann invariants. Our approach will be similar to the one presented in [22] but the final formulas presented in this paragraph have not encountered in literature.

The equations (4) can be rewritten in the following form

$$D_+ R_+ = 0, \quad D_- R_- = 0,$$

where

$$D_+ = \frac{\partial}{\partial t} + \left(u + \frac{1}{\sqrt{\rho D(A)}}\right) \frac{\partial}{\partial x}, \quad D_- = \frac{\partial}{\partial t} + \left(u - \frac{1}{\sqrt{\rho D(A)}}\right) \frac{\partial}{\partial x},$$

$$R_+ = u + \int_{A_0}^A \frac{dz}{\sqrt{\rho D(z)}z}, \quad R_- = u - \int_{A_0}^A \frac{dz}{\sqrt{\rho D(z)}z}.$$

After integration we obtain

$$R_+ = u + \frac{2}{n\sqrt{\rho D_0}}(A^{n/2} - A_0^{n/2}), \quad R_- = u - \frac{2}{n\sqrt{\rho D_0}}(A^{n/2} - A_0^{n/2}). \quad (26)$$

We consider only subsonic flows  $|u| \ll \frac{1}{\sqrt{\rho D(A)}}$  then  $R_+$  is forward traveling component while  $R_-$  is traveling in the opposite direction. From (26) we see that any velocity wave is composed from the two components  $R_+, R_-$ , more exactly  $u = \frac{1}{2}(R_+ + R_-)$ . For the case of the sole forward wave we need to remove the backward component, we set  $R_- = 0$ , then

$$R_+ = 2u, \quad R_- = 0,$$

$$u = \int_{A_0}^A \frac{dz}{\sqrt{\rho D(z)}z}$$

and for the backward wave

$$R_+ = 0, \quad R_- = 2u,$$

$$u = - \int_{A_0}^A \frac{dz}{\sqrt{\rho D(z)}z}.$$

Finally, integrating the right-hand sides of the expressions for the velocities we obtain for the forward and the backward waves respectively

$$u = \pm \frac{2}{n\sqrt{\rho D_0}}(A^{n/2} - A_0^{n/2}). \quad (27)$$

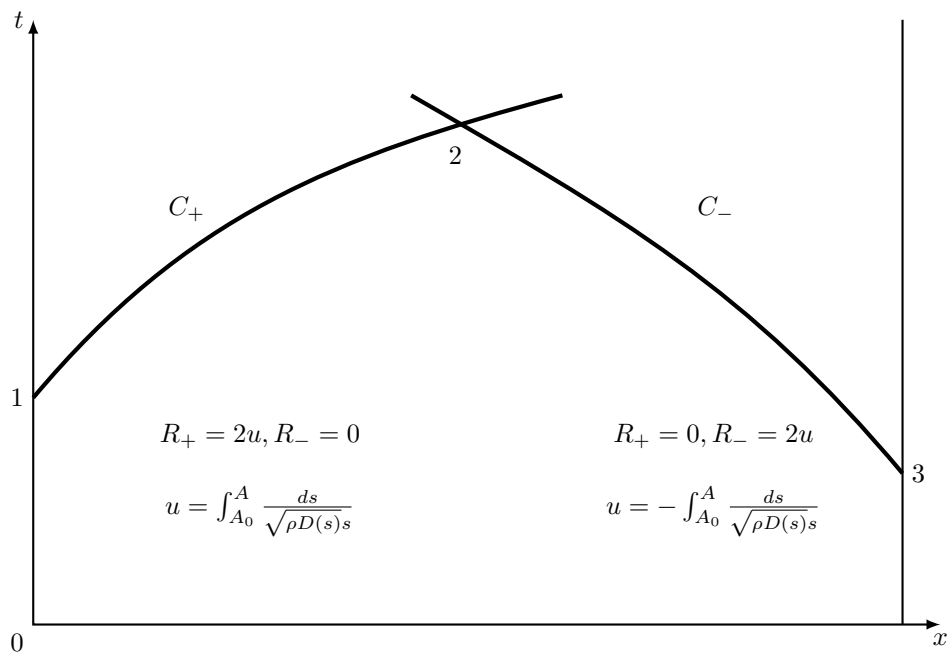


Figure 4: The forward and backward waves starting from the points 1 and 3 travel along the corresponding characteristic curves  $C_+, C_-$  and meet at the point 2.

Let us remember that the pressure can be expressed via vessel cross-section area  $A$  using the relation (3)

$$p = p_0 + \frac{1}{nD_0}(A^n - A_0^n).$$

Now we consider the wave at the point 2 composed of the forward and backward waves starting from the points 1 and 3 (Fig. 3). Let us denote the total blood pressure, the blood velocity and the vessel cross-section area of the composed wave at the point 2 as  $p, u, A$ . Our goal is to separate this wave into the forward and the backward components, or to express the blood pressure of the forward wave  $p_+$  and the backward wave  $p_-$  in terms of  $p, u$ . Using (3) we can express the Riemann invariants in (26) in terms of  $u, p$

$$R_+(u, p) = u + \frac{2}{n\sqrt{\rho D_0}}h(p), \quad R_-(u, p) = u - \frac{2}{n\sqrt{\rho D_0}}h(p), \quad (28)$$

where  $h(p) = \sqrt{nD_0(p - p_0) + A_0^n - A_0^{n/2}}$ . Moreover we can invert this relations and express  $u, p$  in terms of  $R_+, R_-$

$$p(R_+, R_-) = p_0 + \frac{1}{nD_0} \left\{ \left( \frac{n\sqrt{\rho D_0}}{4}(R_+ - R_-) + A_0^{n/2} \right)^2 - A_0^n \right\}, \quad (29)$$

$$u(R_+, R_-) = \frac{R_+ + R_-}{2}. \quad (30)$$

Now let us remember that the forward traveling wave is defined by the condition  $R_- = 0$  while the backward wave is defined by  $R_+ = 0$ . Then we deduce that

$$p_+ = p(R_+, 0) = p_0 + \frac{1}{nD_0} \left\{ \left( \frac{n\sqrt{\rho D_0}}{4}R_+ + A_0^{n/2} \right)^2 - A_0^n \right\}, \quad (31)$$

$$p_- = p(0, R_-) = p_0 + \frac{1}{nD_0} \left\{ \left( -\frac{n\sqrt{\rho D_0}}{4}R_- + A_0^{n/2} \right)^2 - A_0^n \right\}. \quad (32)$$

We substitute the relations (28) for  $R_+ = R_+(u, p), R_- = R_-(u, p)$  in (31)-(32) and after some algebra we obtain the full nonlinear wave-separation formulas

$$\Delta p_+(u, p) = \frac{\rho c_0^2}{2} \left\{ \frac{2}{n}g(\Delta p) + \frac{u}{c_0} \right\} \left\{ 1 + \frac{1}{4}g(\Delta p) + \frac{nu}{8c_0} \right\}, \quad (33)$$

$$\Delta p_-(u, p) = \frac{\rho c_0^2}{2} \left\{ \frac{2}{n}g(\Delta p) - \frac{u}{c_0} \right\} \left\{ 1 + \frac{1}{4}g(\Delta p) - \frac{nu}{8c_0} \right\}, \quad (34)$$

where

$$g(\Delta p) = \sqrt{\frac{n\Delta p}{\rho c_0^2} + 1} - 1$$

and  $\Delta p = p - p_0, \Delta p_{\pm} = p_{\pm} - p_0$ . If we expand  $g(\Delta p)$  in Taylor series on  $\Delta p$  and keep only the first order term then  $g(\Delta p) \approx \frac{n\Delta p}{2c_0^2}$ . Therefore the linear

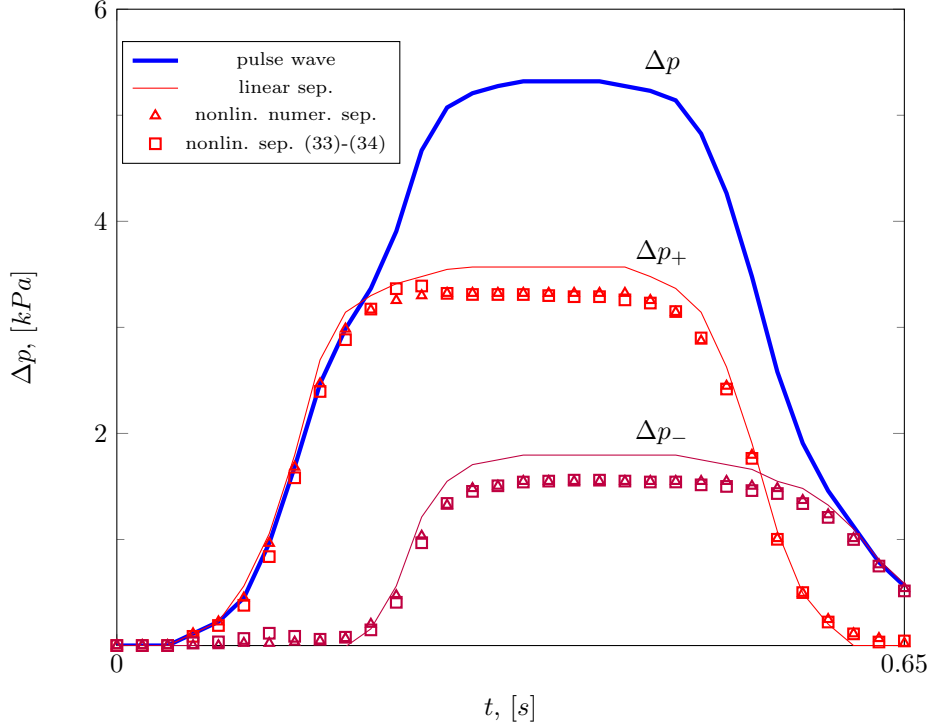


Figure 5: The pressure pulse wave (thick upper line, borrowed from [23]) and its separation in the forward and the backward components for  $n = 4, c_0 = 4m/s, \rho = 1060kg/m^3$ . The squared symbols correspond to the results obtained using the nonlinear wave separation formulas (33)-(34), the other waves are obtained using the classic linear method and the non-linear numerical approach (lines without markers and the triangle symbols respectively) from [23]. The both nonlinear methods show very close results.

approximation of (33)-(34) gives the classical linear wave-separation formulas [11]

$$\Delta p_+(u, p) = \frac{\rho c_0^2}{2} \left( \frac{\Delta p}{\rho c_0^2} + \frac{u}{c_0} \right), \quad \Delta p_-(u, p) = \frac{\rho c_0^2}{2} \left( \frac{\Delta p}{\rho c_0^2} - \frac{u}{c_0} \right).$$

Keeping the quadratic terms in the expressions (33)-(34) leads to the following simplified nonlinear wave separation formulas

$$\Delta p_+(u, p) = \frac{\rho c_0^2}{2} \left\{ \left( \frac{\Delta p}{\rho c_0^2} + \frac{u}{c_0} \right) + \frac{n}{8} \left[ - \left( \frac{\Delta p}{\rho c_0^2} \right)^2 + 2 \frac{u}{c_0} \frac{\Delta p}{\rho c_0^2} + \left( \frac{u}{c_0} \right)^2 \right] \right\}, \quad (35)$$

$$\Delta p_-(u, p) = \frac{\rho c_0^2}{2} \left\{ \left( \frac{\Delta p}{\rho c_0^2} - \frac{u}{c_0} \right) + \frac{n}{8} \left[ - \left( \frac{\Delta p}{\rho c_0^2} \right)^2 - 2 \frac{u}{c_0} \frac{\Delta p}{\rho c_0^2} + \left( \frac{u}{c_0} \right)^2 \right] \right\}. \quad (36)$$

The results of the analytical study can be validated on the data from literature. We compare the wave profiles calculated using the formulas (33)-(34)

with the results presented in [23] where the nonlinear wave separation technique was based on the calculation of the infinitesimal changes of the forward and the backward waves  $dp_{\pm} = \pm \frac{\rho c_{\pm}}{2} dR_{\pm}$ , where  $c_{\pm} = u \pm c(p)$ ,  $c(p) = \sqrt{(n/\rho)\Delta p + c_0^2}$ . The equations for  $R_{\pm}$  :  $dR_{\pm}/dt + c_{\pm}dR_{\pm}/dx = 0$  are solved numerically using the locally conservative Galerkin method. The details about the applied numerical method can be also found in [25],[26]. The numerical approach from [23] and the present approach give very close results since the same equations are solved. The comparison of the methods shows that the discrepancies are negligible except of some points (Fig. 4).

The form of the simplified nonlinear wave separation expressions (35)-(36) allows to assess the influence of the nonlinear effects. Typically  $\Delta p > \rho c_0 u$ , therefore the term  $-(n/8)(\Delta p/\rho c_0^2)^2$  is dominant among the nonlinear terms. Obviously, this term suppresses the amplitudes of forward and backward waves. This feature is illustrated in Fig 4. The effect can be observed in several cases. Firstly, for high pressures the vessel's wall compliance becomes low and this effect can be modeled using  $n \gg 1$  and then the nonlinear effects should be taken in account if  $c_0$  remains average for the such pressures. On the other hand, for the classical Hooke law  $n = 1/2$  the nonlinear effects can be significant for moderate velocities  $c_0 = \frac{\sqrt{A}}{\rho D_0} = \frac{2\sqrt{\pi}Eh}{3\rho A_0}$  which can be potentially observed in a situation if the Young's modulus  $E$  and the wall thickness  $h$  are small and the vessel is compliant.

## Conclusion

The nonlinear 1D equations for the inviscid blood flow were investigated analytically. The viscoelastic terms in the vessel wall-pressure response were excluded in the analysis, the unperturbed luminal area was constant alongside the considered vessels. Closed expressions for nonlinear forward (or backward) waves for a class of particular initial-boundary conditions (including triangle shape profiles) has been derived assuming that the terms  $(\Delta A/A_0)^2$  (the quadratic terms on the relative systolic change of the vessel's cross-section area) are small. As a result, the shock formation conditions have been obtained. In addition, the analytical expressions for the wave separation into the forward and backward components were deduced.

The introduction of friction in the simplest form results in the addition of  $\frac{frict}{\rho A}$  terms in the right side of the second equation (4) , where *frict* is the wall friction force proportional to  $-\nu u$  and  $\nu$  is the blood viscosity. For the Eqs (4) with the friction included the forward traveling wave cannot be taken in the form (5). Qualitatively we suppose that the friction will prevent the appearance of shocks if the initial wave is too flat [32]. Mathematically this problem can be considered as the asymptotic expansion on  $\nu$  which is an interesting subject the future study.

The analytical nonlinear pulse wave expression could be used in the evaluation of the central pressure based on the pressure forms in other arteries. The principal method for the assessment of the central (aortic) blood pressure

from the applanation tonometry measurements in brachial (or radial) arteries is based on the application of transfer functions [28]-[30]. This function matches the Fourier harmonics of the radial (brachial) and the aortic pressures and is derived using the regression analysis. As the shape of the nonlinear pressure wave and its change during the propagation can be obtained analytically then the following approach could be tested. As a first step the separation of the blood pressure measured in a radial artery into forward and backward components could be performed using the pressure profiles only [12]. Next, we estimate the free parameters  $t_0, x_0$  (see (25)) for which the analytical profile has the best fit with the assessed forward component. Finally, the aortic pressure can be recovered by application of the shift in variables  $(t, x) \rightarrow (t - \delta t, x - \delta x)$  where  $(\delta t, \delta x)$  are the approximate time and distance traveled by the pulse wave from the aortic root to the vessel under the consideration.

I wish to thank Oleg A. Rogozin for the discussions.

The work was supported by Russian Foundation for Basic Research, grant No 18-01-00899.

## References

## References

- [1] T. Hughes, J. Lubliner, On the one-dimensional theory of blood flow in the larger vessels, *J. Math. Biosci.* 18 (1973) 161–170.
- [2] C. Taylor, M. Draney, Experimental and computational methods in cardiovascular fluid mechanics, *Annu. Rev. Fluid Mech.* 36 (2004) 197–231.
- [3] S. Sherwin, V. Franke, J. Peiró and K. Parker, One-dimensional modelling of a vascular network in space-time variables, *J. Engng. Maths.* 47 (2003) 217–250.
- [4] N. Stergiopoulos, D. Young, T. Rogge, Computer simulation of arterial flow with applications to arterial and aortic stenoses, *J. Biomech.* 25 (1992) 1477–1488.
- [5] Y. Huo and G. Kassab, Pulsatile blood flow in the entire coronary arterial tree: theory and experiment, *Am. J. Physiol. Heart Circ. Physiol.* 291 (2006) H1074-H1087.
- [6] Y. Huo and G. Kassab, A hybrid one-dimensional/Womersley model of pulsatile blood flow in the entire coronary arterial tree, *Am. J. Physiol. Heart. Circ. Physiol.* 292 (2007) H2623–H2633.
- [7] P. Reymond, F. Merenda, F. Perren, D. Rüfenacht, N. Stergiopoulos, Validation of a one-dimensional model of the systemic arterial tree, *Am. J. Physiol. Heart Circ. Physiol.* 297 (2009) H208-H222.



- [8] J. Alastruey, A. Khir, K. Matthys, P. Segers, S. Sherwin, P. Verdonck, K. Parker, J. Peiró, Pulse wavepropagation in a model human arterial network: Assessment of 1-D visco-elastic simulations against in vitro measurements, *J.Biomech.* 44 (2011) 2250–2258.
- [9] L. Formaggia, J. Gerbeau, F. Nobile, A. Quarteroni, On the coupling of 3D and 1D Navier-Stokes equations for flow problems in compliant vessels, *Comp. Meth. in Appl. Mech. Engng.* 191 (2001) 561–582.
- [10] H. Lamb, *Hydrodynamics*, Dover Publicaion, New York, 1945.
- [11] N. Westerhof, P. Sipkema, G. van den Bos Elzinga G, Forward and backward waves in the arterial system, *Cardiovasc. Res.* 6 (1972) 648–656.
- [12] B. Westerhof, I. Guelen, N. Westerhof, J. Karemaker, A. Avolio, Quantification of Wave Reflection in the Human Aorta From Pressure Alone A Proof of Principle, *Hypertension* 48 (2006) 595–601.
- [13] A. Hughes, K. Parker, Forward and backward waves in the arterial system: impedance or wave intensity analysis? *Med. Biol. Eng. Comput.* 47 (2009) 207–210.
- [14] N. Westerhof, P. Segers, B. Westerhof, Wave Separation, Wave Intensity, the Reservoir-Wave Concept, and the Instantaneous Wave-Free Ratio Presumptions and Principles, *Hypertension* 66 (2015) 93–98.
- [15] A. Khir, A. O’ Brien, J. Gibbs, K. Parker, Determination of wave speed and wave separation in the arteries, *J. Biomech.* 34 (2001) 1145–1155.
- [16] G. Gamble, J. Zorn, G. Sanders, S. MacMahon, N. Sharpe, Estimation of arterial stiffness, compliance, and distensibility from M-mode ultrasound measurements of the common carotid artery, *Stroke* 25 (1994) 11–16.
- [17] L. Forbes, On the evolution of shock-waves in mathematical models of the aorta, *J. Austral. Math. Soc. B* 22 (1981) 257–269.
- [18] G. Rudinger, Shock Waves in Mathematical Models of the Aorta, *J. Appl. Mech.* 37 1970 34–37.
- [19] B. Brook, S. Falle, T. Pedley, Numerical solutions for unsteady gravity-driven flows in collapsible tubes: evolution and roll-wave instability of a steady state, *J. Fluid Mech.* 396 (1999) 223–256.
- [20] K. Parker, C. Jones, Forward and Backward Running Waves in the Arteries: Analysis Using the Method of Characteristics, *J. Biomech Eng.* 112 (1990) 322–326.
- [21] F. Pythoud, N. Stergiopoulos, J. Meister, Separation of Arterial Pressure Waves Into Their Forward and Backward Running Components, *J. Biomech. Eng.* 118 (1996) 295–301.

- [22] F. Pythoud, N. Stergiopoulos, C. Bertram, J. Meister, Effects of friction and nonlinearities on the separation of arterial waves into their forward and backward components, *J. Biomech.* 29 (1996) 1419–1423.
- [23] J. Mynard, M. Davidson, D. Penny, J. Smolich, Non-linear separation of pressure, velocity and wave intensity into forward and backward components, *Med. Biol. Eng. Comput.* 50 (2012) 641–648.
- [24] Large Blood Vessels. 1.1 Introduction The Cardiovascular System. <http://www.maths.gla.ac.uk/~xl/NAH-background.pdf>, X. Luo (accessed 18 March 2018).
- [25] J. Mynard, P. Nithiarasu, A 1D arterial blood flow model incorporating ventricular pressure, aortic valve and regional coronary flow using the locally conservative Galerkin (LCG) method, *Commun. Numer. Meth. Engng.* 24 (2008) 367–417.
- [26] J. Mynard, M. Davidson, D. Penny, J. Smolich, A numerical model of neonatal pulmonary atresia with intact ventricular septum and RV-dependent coronary flow, *Int. J. Numer. Meth. Biomed. Engng.* 26 (2010) 843–861.
- [27] N. Stergiopoulos, Y. Tardy, J. Meister, Nonlinear separation of forward and backward running waves in elastic conduits, *J. Biomech.* 26 (1993) 201–209.
- [28] M. Karamanoglu, M. O’Rourke, A. Avolio, R. Kelly, An analysis of the relationship between central aortic and peripheral upper limb pressure waves in man, *Eur. Heart J.* 14 (1993) 160–167.
- [29] C. Chen, E. Nevo, B. Fetis, P. Pak, F. Yin, W. Maughan, D. Kass, Estimation of central aortic pressure waveform by mathematical transformation of radial tonometry pressure. Validation of generalized transfer function, *Circulation* 95 (1997) 1827–1836.
- [30] A. Pauca, M. O’Rourke, N. Kon, Prospective Evaluation of a Method for Estimating Ascending Aortic Pressure From the Radial Artery Pressure Waveform, *Hypertension* 38 (2001) 932–937.
- [31] G. Langewouters, K. Wesseling, W. Goedhard, The static elastic properties of 45 human thoracic and 20 abdominal aortas in vitro and the parameters of a new model, *J. Biomech.* 17 (1984) 425–435.
- [32] G. Whitham, *Linear and Nonlinear waves*, John Wiley & Sons, New York, 1999.

## Appendix. Distensibility and Hooke law

Consider the pressure-area relationship (3)

$$p = p_0 + \frac{1}{nD_0}(A^n - A_0^n).$$

If  $n = 1/2$  the Hooke law is derived in the following form [8]

$$p = p_0 + \frac{4\sqrt{\pi}Eh}{3A_0}(\sqrt{A} - \sqrt{A_0}), \quad (37)$$

where  $E$  is the Young's modulus,  $h$  is the vessel wall thickness. The viscoelastic terms are not considered in the present study. In general case the Young's modulus is not constant but is an increasing function of blood pressure  $E = E(p)$  [31]. This fact means that the stiffness of an artery increases for high pressures. In contrast to the Hooke law  $A(p) \sim p^2$ , for the real arteries like aorta (non-constant Young's modulus) the saturation of vessel distension is observed, this effect can be modeled using the arctangent function  $A(p) \sim \arctan(p)$ . The saturation effects appear for pressures close to  $200 \text{ mmHg}$ , for pressures in a range  $100 - 200 \text{ mmHg}$  we observe that  $\frac{dA}{dp}$  is decreasing function of  $p$ , see Fig. 4 in [31]. This feature can be recovered in the expressions (3) if we assume that  $n > 1$  ( $A \sim p^{1/n}$ ).

## Appendix 2. General solution for the sole forward wave

Recall the equation (4)

$$\frac{\partial A}{\partial t} + \frac{1}{\sqrt{\rho D_0}} \left( \left(1 + \frac{2}{n}\right) A^{n/2} - \frac{2}{n} A_0^{n/2} \right) \frac{\partial A}{\partial x} = 0,$$

the formal solution along the characteristics is

$$A = \text{const}, \quad \frac{dt}{dx} = \frac{n\sqrt{\rho D_0}}{(n+2)A^{n/2} - 2A_0^{n/2}},$$

where  $dt/dx > 0$  since  $A \geq A_0$  for any values of  $t, x$ . Note that  $A$  is constant on the characteristics  $t(x)$ . The characteristics depend on the different values of the parameter  $s$ ,  $t(0) = s$ . Then, after integration we have

$$A = f(s), \quad t = \frac{n\sqrt{\rho D_0}}{(n+2)f(s)^{n/2} - 2A_0^{n/2}}x + s, \quad (38)$$

where the function  $f(s)$  should be defined from the boundary conditions. Replacing the parameter  $s$  by  $f^{-1}(A)$  in the second equation (38) we obtain

$$A = f \left( t - \frac{n\sqrt{\rho D_0}x}{(n/2)A^{n/2} - 2A_0^{n/2}} \right).$$

For the boundary conditions (8) we conclude that  $f(s)$  takes the form

$$f(s) = A_0 + as,$$

then

$$A = A_0 + a \left( t - \frac{n\sqrt{\rho D_0}x}{(n+2)A^{n/2} - 2A_0^{n/2}} \right). \quad (39)$$

The explicit analytical expression for  $A$  can not be obtained from the equation (39) in the case of general  $n$ .